

Short communication

## Micro-hotplates—A platform for micro-solid oxide fuel cells

Daniel Beckel<sup>a,\*</sup>, Danick Briand<sup>b</sup>, Anja Bieberle-Hütter<sup>a</sup>, Jérôme Courbat<sup>b</sup>,  
Nicolaas F. de Rooij<sup>b</sup>, Ludwig J. Gauckler<sup>a</sup>

<sup>a</sup> *Nonmetallic Inorganic Materials, Department of Materials, ETH Zürich, Wolfgang-Pauli-Str. 10, CH-8093 Zürich, Switzerland*

<sup>b</sup> *Institute of Microtechnology, University of Neuchâtel, Rue Jaquet-Droz 1, P.O. Box 528, CH-2002 Neuchâtel, Switzerland*

Received 10 April 2006; received in revised form 17 November 2006; accepted 28 December 2006

Available online 13 January 2007

### Abstract

Special high temperature micro-hotplates were investigated for their potential use as a technology platform for miniaturized solid oxide fuel cells (SOFCs). To evaluate the compatibility of these hotplates with typical SOFC materials and processing techniques, spray pyrolysis was used for the deposition of an SOFC cathode material ( $\text{La}_{0.6}\text{Sr}_{0.4}\text{Co}_{0.2}\text{Fe}_{0.8}\text{O}_3$ , LSCF) onto the micro-hotplate. The resulting microstructures and the electrical conductivity of the thin film (thickness  $\sim 500$  nm) were characterized. Post-deposition annealing in external furnaces as well as using the integrated heater of the micro-hotplate confirmed that these micro-hotplates are suitable for a maximum operation temperature of  $800^\circ\text{C}$  and a long-term operation at  $600^\circ\text{C}$ . Very fast heating and cooling rates of several  $100^\circ\text{C min}^{-1}$  were achieved using the micro-hotplate as a heater, allowing fast processing and aging tests. Bending of the micro-hotplate was found to be critical to the integrity of the thin film, which coats the micro-hotplate. Bending might be reduced using other membrane materials.

These membranes are potential components for a micro-SOFC in which the integrated heater is used for start-up operation of the fuel cell.

© 2007 Elsevier B.V. All rights reserved.

**Keywords:** Solid oxide fuel cell (SOFC); Micro-hotplate; Thin film; Spray pyrolysis; Lanthanum strontium cobalt iron oxide (LSCF); Thermal cycling

### 1. Introduction

Micro-hotplates generally consist of a thin ( $\sim 1$   $\mu\text{m}$ ) dielectric membrane suspended over an opening in a silicon substrate [1–4]. In microsystems technology, such hotplates are mainly used for sensor applications where the sensing material is deposited onto the membrane and an electrical signal is conducted using contacts integrated on the hotplate [1,3]. A heater is also integrated in the hotplate, which typically operates at temperatures around  $200$ – $400^\circ\text{C}$  [5]. In recent years, micro-hotplates operating at temperatures higher than  $500^\circ\text{C}$  have been developed for various applications, such as sensors, actuators, infrared sources, micro-reactors or to perform annealing of films or chemical vapor deposition (CVD) on-chip [1,3,6,7].

In the field of solid oxide fuel cells (SOFCs), development currently trends towards lower operating temperatures (from  $800$ – $1000^\circ\text{C}$  down to  $500$ – $700^\circ\text{C}$ ) [8–10] and to miniaturization of SOFCs [11]. Reduction of the operating temperature is

intended to reduce material degradation and facilitate sealing of SOFCs. Miniaturization of SOFCs enables new applications such as battery replacement [11]. With thin film components the ohmic resistances of the cell's components are reduced, allowing operation at lower temperatures.

These developments led to the situation in which SOFCs and micro-hotplates are now able to operate at similar temperatures, i.e. around  $500^\circ\text{C}$ . Thus, we investigate a micro-hotplate as platform for a micro-SOFC with an integrated heater that can be used for start-up operation as well as for processing of SOFC components. Electrical contacts and a thermocouple can also be integrated.

To evaluate the feasibility of this approach, first the compatibility of the thin film components with the micro-hotplates needed to be clarified. Contacting of the micro-SOFC is simplified if all three components (cathode, electrolyte and anode) are deposited onto one side of the micro-hotplate. Therefore, we deposited in this study the cathode, which is the first layer, directly onto the high temperature micro-hotplate [1]. We chose  $\text{La}_{0.6}\text{Sr}_{0.4}\text{Co}_{0.2}\text{Fe}_{0.8}\text{O}_3$  (LSCF) as cathode material and spray pyrolysis [12,13] as deposition technique. The microstructural and mechanical integrity of the LSCF thin film is investigated

\* Corresponding author. Tel.: +41 44 632 3763; fax: +41 44 632 1132.  
E-mail address: [Daniel.Beckel@mat.ethz.ch](mailto:Daniel.Beckel@mat.ethz.ch) (D. Beckel).

by high resolution microscopy. We also evaluated the electrical conductivity of the thin film on the micro-hotplate. Realization of an entire micro-SOFC would then require deposition of the electrolyte and the anode on top of the cathode plus openings in the micro-hotplate membrane to allow gas access to the cathode.

## 2. Experimental

The LSCF thin films were deposited by spray pyrolysis onto micro-hotplates. Contacting for the electrical measurements was done via patterned electrodes of defined geometry, which were fabricated on the micro-hotplates prior to thin film deposition. A detailed description of each process step is given in the following sections.

### 2.1. Micro-hotplate design and fabrication

The micro-hotplates were fabricated on silicon wafers. They consisted of a dielectric membrane in which a platinum (Pt) heater was embedded and covered on top by electrodes (Fig. 1A). The heater was made of platinum with a tantalum (Ta) adhesion layer (225 nm thick). The Pt/Ta film was patterned using a lift-off process. In this process a sacrificial lift-off resist layer (LOR MicroChem Corp.) was patterned using a standard S1823 photoresist (Shipley Corp.) on top. After Pt/Ta deposition the sacrificial layer was removed, leaving the Pt/Ta only in the areas where an opening was patterned in the sacrificial layer. More details on the lift-off process are described elsewhere [14]. Two low-stress silicon nitride (SiN) films deposited by low pressure chemical vapor deposition (LPCVD) formed the thermally insulated 1.0  $\mu\text{m}$ -thick membrane of the micro-hotplate. Dense Pt/Ta electrodes 150 nm thick were patterned on top of the membrane using the same lift-off process described above. The dielectric membrane was released using back-side bulk wet etching of the silicon wafer. More details about the fabrication process can be found in reference [1].

The membrane has an area of 1.0 mm  $\times$  1.0 mm, and the areas covered by the double meander heater and the electrodes were 530  $\mu\text{m}$   $\times$  530  $\mu\text{m}$  and 400  $\mu\text{m}$   $\times$  400  $\mu\text{m}$ , respectively. The electrodes were used to contact the film for the electrical measurements with defined geometries. In a complete fuel cell, current collectors could be fabricated the same way. The design included different geometries for the shape of the electrodes in

a four-point configuration. The electrodes were made of four square contact pads with two different gaps and widths. One design has square pads contacts 180  $\mu\text{m}$  wide and a gap between the square contacts of 40  $\mu\text{m}$ . The other design has square contacts 50  $\mu\text{m}$  wide and a gap between the different square contacts of 300  $\mu\text{m}$  as shown in Fig. 1B.

The temperature reached at the centre of the micro-hotplates as a function of the input power was calibrated using a micro-thermocouple, type S, made of Pt–PtRh wires with a diameter of 1.3  $\mu\text{m}$  [15]. A temperature of 600  $^{\circ}\text{C}$  was reached at a low power of 120 mW.

### 2.2. Thin film deposition

LSCF thin films were deposited by air-pressurized spray pyrolysis. For the spray solution, a mixture of metal salts with a molar ratio of  $\text{LaNO}_3 \cdot 6\text{H}_2\text{O}:\text{SrCl}_2 \cdot 6\text{H}_2\text{O}:\text{Co}(\text{NO}_3)_2 \cdot 6\text{H}_2\text{O}:\text{Fe}(\text{NO}_3)_3 \cdot 9\text{H}_2\text{O} = 3:2:1:4$  (all from Fluka with purity >98%) and a total salt concentration of 0.02 mol l<sup>-1</sup> was dissolved in a solvent composition of 1/3 (volume fraction) ethanol (Scharlau and Merk, purity >99.5%) and 2/3 diethylene glycol monobutyl ether (from Fluka and Acros Organic, purity  $\geq$ 98%). The resulting solution was pumped (peristaltic pump: Ismatec MS Reglo or syringe pump: Razell Scientific Instruments A 99) with a solution flow rate of 30 ml h<sup>-1</sup> through a nozzle (Badger Air-brush Model 150), which was located 20 cm above the micro-hotplate and atomized by air pressure of 1 bar. These droplets were sprayed through a shadow mask onto the micro-hotplate using an external hotplate at around 270  $^{\circ}\text{C}$  in order to evaporate the solvent. The micro-hotplate was fixed in an aluminum holder that also held and aligned the shadow mask. At these conditions a spraying time of 60 min resulted in a layer thickness of  $\sim$ 500 nm to  $\sim$ 1  $\mu\text{m}$ .

Alternatively, the film was deposited onto the micro-hotplate using the integrated heater also at 270  $^{\circ}\text{C}$ . No masks were needed, because the film was only deposited in the hot area. Outside the hot area the liquid spray solution accumulated and was rinsed after deposition. Care has to be taken that the accumulating liquid solution outside the hot area does not short-circuit the wiring, or suddenly floods the chip.

After deposition the film is amorphous and can be crystallized in an additional annealing step using the integrated heater or using an external furnace. Annealing was typically done at 600  $^{\circ}\text{C}$  in air.

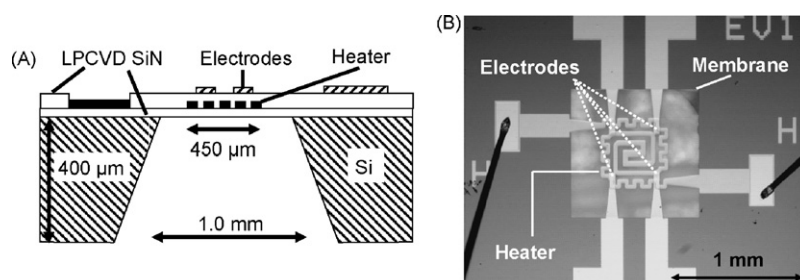


Fig. 1. (A) Schematic cross-section view of a micro-hotplate made of a Pt heater in between two SiN thin films, covered on top by electrodes. (B) Top view of micro-hotplate with membrane and heater.

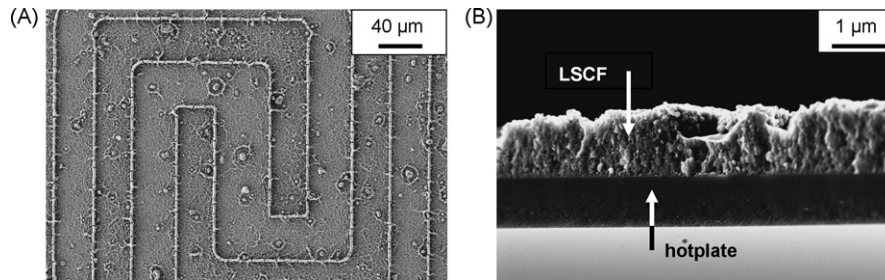


Fig. 2. SEM micrographs of LSCF thin films on micro-hotplates. (A) Top view and (B) cross-section.

### 2.3. Thin film characterization

The microstructure was characterized by light microscopy (NIKON Optiphot 150) and scanning electron microscopy (SEM Leo 1530 and Philips XL30 ESEM-FEG). The film thickness was determined from cross-section micrographs of the film on the micro-hotplate membrane and used to determine the electrical conductivity of the LSCF coating. The membrane deformation of the uncoated and coated micro-hotplates as a function of the input power was measured using an optical profilometer (UBM GmbH) with a resolution of 10 nm.

The micro-hotplate's maximum power before breakdown was characterized using the Hewlett Packard 4155 A semiconductor parameter analyser. The applied voltage of the device increased from 0 to 10 V with steps of 0.05 V and an integration time of 100 ms.

The electrical conductivity of the LSCF films deposited onto the micro-hotplate was measured in air in two-point and four-point probe configurations using the integrated Pt electrodes. The silicon chip was glued to a TO-5 socket and the contact pads of the heater and electrodes connected using wire bonding. The HP 6644A dc power supply was used to warm up the chip using the integrated heater. The control of the power supplied to the heater and the monitoring of the electrical resistance of the LSCF films from the multimeter HP 34401A were performed using Labview.

The electrical conductivity of the LSCF films deposited onto the sapphire bulk substrates, which served as reference samples, was measured in air in a modified tubular furnace. A four-point setup was used and the data was recorded with a multimeter (Keithley 2000) controlled through the Labview software installed on a computer. Flattened Pt wires (Johnson Matthey) were used as electrodes. To ensure good adhesion of the electrodes, sputtered Pt and Pt paste (Heraeus) connected the electrodes to the film. Additionally, the electrodes were glued to the substrate outside the film using ceramic glue (Firag) with some Pt powder (Johnson Matthey) added for improved adhesion.

## 3. Results and discussion

### 3.1. Microstructure

A typical SEM micrograph showing the top view and the cross-section of an LSCF thin film deposited onto a micro-hotplate is shown in Fig. 2. The ridges found in the top view

were built during the film deposition following the topology of the micro-hotplate, e.g. the heater and the electrodes. They also form the round features visible in Fig. 2A. The mechanism of formation of these ridges is related to spray pyrolysis and is discussed in more detail elsewhere [12,16]. The cross-section image (Fig. 2B) shows that the films are about 1 μm thick and that the microstructure is porous.

Differences in the microstructure are observed with respect to the substrate material, as shown in Fig. 3. In the areas of the membrane where the SiN is covered by the Pt electrodes or where the Pt heater is embedded in the SiN membrane, fewer cracks are found than on areas consisting of SiN only. The reasons are the thermal properties of the substrate materials: if the product of thermal conductivity times heat capacity is large, as is the case for Pt, the heat transfer from the substrate to the droplets during film deposition is fast. That means a larger fraction of the non-uniform sized droplets will show Leidenfrost's phenomenon, i.e. hovering on their own steam, thus they do not contribute to film formation [17]. As a consequence, less material is deposited leading to thinner films, which reduces crack formation. In the case of a pure SiN substrate, the product of thermal conductivity times heat capacity is small and, hence, cracks easily form due to thicker films. By reducing the solution flow rate and deposition time, crack-free films can also be obtained on SiN substrates. However, if materials with strongly different thermal properties are combined in one substrate, the film thickness and thus the occurrence of cracks varies across the substrate. Thus, the design

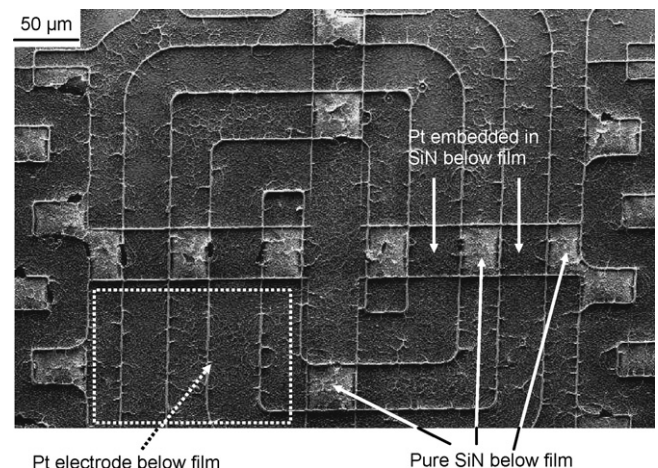


Fig. 3. SEM micrograph of LSCF deposited onto a micro-hotplate consisting of different materials.

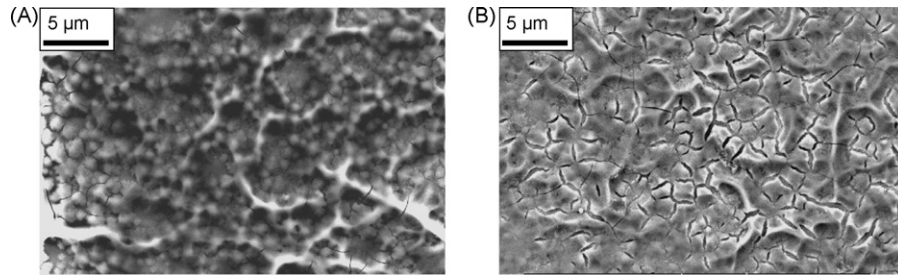


Fig. 4. SEM micrographs of LSCF on micro-hotplates. (A) As-deposited and (B) annealed for 20 min.

of the metallic lines in the heater is important for the coherence of the film.

To observe the microstructure of the films during annealing, the integrated heater of the micro-hotplate was used for different periods and then the microstructure was inspected by SEM. Micrographs at different areas of the sample were taken before annealing and after annealing periods of 5, 20 and 450 min at 600 °C. The surface of an as-deposited film shows round grain-type features with a medium diameter of around 500 nm and rim structures originating from the film formation from droplets, as shown in Fig. 4A. After 5 min of annealing at 600 °C, the round grain-type features of the film disappear and small cracks on the surface of the film are formed. After 20 min (Fig. 4B) or even 450 min annealing, no further changes appear in the microstructure. Generally, fewer cracks are found in the film when the sample is annealed in a furnace and not by using the integrated heater. In this case, the whole chip is at the same temperature and so bending of the membrane is expected to be diminished, improving the integrity of the film. Furthermore, no significant microstructural difference between the films deposited onto micro-hotplates or sapphire substrates was observed if both films were annealed in external furnaces.

When the integrated heater is used during film deposition, small LSCF crystals sometimes are found on top of the thin film. These crystals may be formed from liquid spray solution entering the membrane from the surrounding area, as explained in Section 2. Film quality can be improved by avoiding spill-over of the liquid precursor during deposition.

### 3.2. Mechanical stability

Bending of the micro-hotplates' membrane upon heating was determined for samples with and without coating (namely LSCF and w/o coating, respectively, Fig. 5). Both samples were flat up to 410 °C (LSCF) and 340 °C (w/o coating), respectively. When exceeding these temperatures, increased bending was observed with increasing temperature. Samples with LSCF coating bent less due to increased thickness of the membrane and thus increased stiffness. Further reduction of bending is expected when replacing the SiN used for the micro-hotplate membrane by aluminum oxide (Al<sub>2</sub>O<sub>3</sub>), due to the higher Young's Modulus of Al<sub>2</sub>O<sub>3</sub> of 345–409 GPa [18] versus 230–265 GPa of SiN [19].

A maximum power test of an uncoated pure SiN micro-hotplate shows two failure modes: breaking of the membrane and electro-stress migration of the Pt atoms forming the heater, influenced by the elasticity and the strength of the membrane.

This observation indicates that the membrane deformation and the migration of the Pt atoms are correlated [20]. A difference is noticed in the maximum power values obtained for the different electrode designs investigated. The maximum powers obtained in these testing conditions are 229 and 245 mW for the smaller and the larger electrodes, respectively. These powers can generate high temperature over 800 °C on the micro-hotplate. The fact that the power of 120 mW is enough to heat the device up to 600 °C offers a secure margin for the operation of the coated devices to be annealed on-chip.

### 3.3. Conductivity

In Fig. 6A, the electrical conductivity of an LSCF thin film deposited onto a micro-hotplate is compared to the conductivity from such a film deposited onto a bulk sapphire substrate as reference. The electrical conductivity was measured during annealing of the samples at 600 °C. For the micro-hotplate, the integrated heater was used for annealing, whereas the sample on the bulk substrate was annealed using an external furnace. Both films show increasing conductivity with time with a comparable rate. We attribute this change in conductivity to the increasing amount of crystalline phase fraction in the films with increasing annealing time at 600 °C. As was recently shown for spray pyrolysis films, high temperatures or long annealing times are needed in order to transform all amorphous material into a crys-

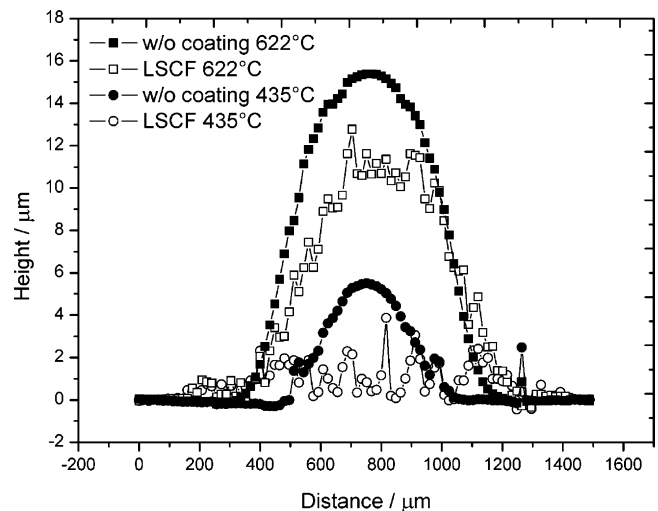


Fig. 5. Bending of micro-hotplates for different temperatures. One sample is coated with LSCF, the other one is without coating (w/o coating).

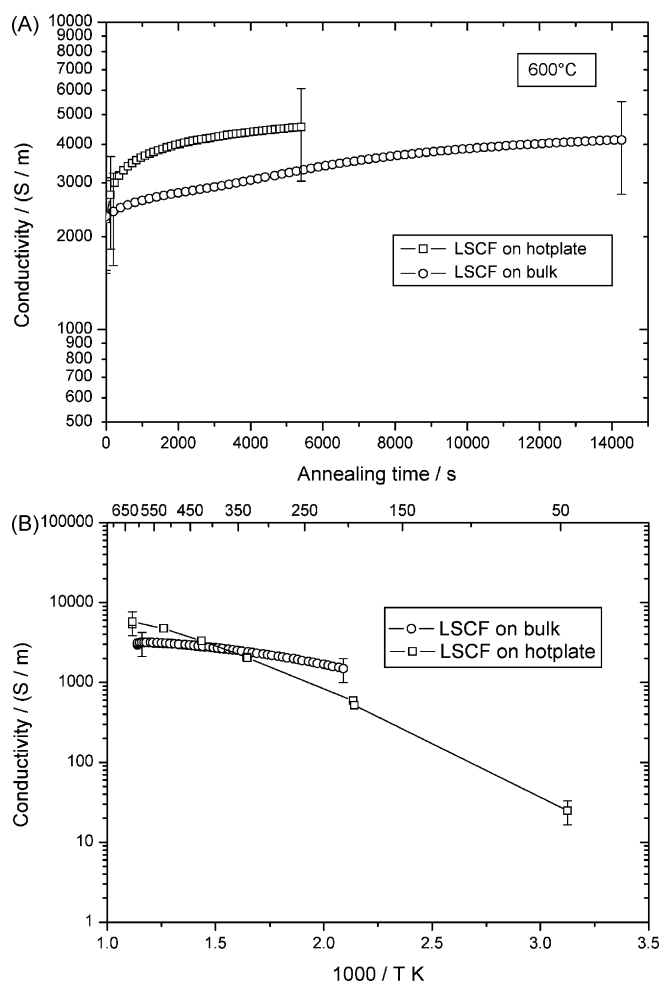


Fig. 6. (A) Electrical conductivity during annealing of LSCF thin films, deposited onto micro-hotplate and onto bulk substrate (sapphire), respectively. (B) Conductivity vs. reciprocal temperature.

talline phase [21]. The crystalline material has a higher electrical conductivity than the amorphous.

After about 30 min of annealing, the film deposited onto the micro-hotplate already reached the conductivity that the film on the bulk substrate reached after 4 h of annealing, meaning the film on the flexible micro-hotplate crystallized faster than the film constrained by the rigid sapphire substrate. A similar relation between microstrain and crystallinity has recently been reported [21].

In Fig. 6B, the electrical conductivities of two LSCF films are compared, which were both already annealed using an external furnace, but again one film was deposited onto a micro-hotplate and one onto a bulk sample as a reference. The electrical conductivities for different temperatures during cooling were measured using the integrated heater for the micro-hotplate-based sample and the furnace for the reference sample. With the sample deposited onto a bulk substrate no cooling rate faster than  $3\text{ }^{\circ}\text{C min}^{-1}$  was realized due to the latent heat of the furnace. The micro-hotplate reacted immediately to a change in input power, thus it was cooled stepwise. Both samples show similar electrical conductivity at the target temperature, indicating that the LSCF thin film stays coherent on the micro-hotplate. However,

the activation energy differs by a factor of about two. The LSCF thin film on the bulk substrate shows an activation energy of 0.12 eV in the temperature range of 200–500  $^{\circ}\text{C}$ , which is close to the one reported in literature of 0.10 eV for bulk LSCF in the temperature range of 100–500  $^{\circ}\text{C}$  [22]. In contrast, the LSCF thin film on the micro-hotplate shows an activation energy of 0.26 eV in the range of 200–500  $^{\circ}\text{C}$ . The reason for the difference might be a loss of film integrity upon cooling, which caused higher resistance and thus higher apparent activation energy.

For LSCF thin films on bulk substrates, a low degradation of 0.5–1% increase in resistance per 100 h was found when the samples were kept at 600  $^{\circ}\text{C}$ . However, for LSCF thin films on micro-hotplates the same increase in resistance was found in about 20 h. Based on this pronounced difference between both types of samples, the degradation is most likely not only caused by the thin film material itself. Instead, it may be associated with the entire system. As already pointed out in Section 3.2, bending of the hotplate might affect the integrity of the thin film. Furthermore, the mismatch in thermal expansion coefficient (TEC) of  $\alpha = 1.6 \times 10^{-6}\text{ K}^{-1}$  [23] for the membrane material (SiN) and  $\alpha = 14 \times 10^{-6}\text{ K}^{-1}$  [24] for the thin film might also be critical to the film. It is expected that the performance can be significantly improved by using  $\text{Al}_2\text{O}_3$  as the membrane material. Besides a reduction of bending, the TEC of  $\text{Al}_2\text{O}_3$  with  $\alpha = 7.8 \times 10^{-6}\text{ K}^{-1}$  [25] is also beneficial and should help to maintain the performance for longer time.

Thermal cycling is a critical issue for operation of SOFCs and was addressed with the following experiment. A sample deposited onto a micro-hotplate was exposed to several rapid ( $10\text{ }^{\circ}\text{C s}^{-1}$ ) temperature cycles from room temperature to 620  $^{\circ}\text{C}$ . The resistance was recorded versus time as shown in Fig. 7. The vertical lines indicate fast thermal cycling steps to room temperature resulting in high resistance; the other resistance values are taken at 620  $^{\circ}\text{C}$ . The resistance increases with every cooling and heating cycle, but stays in the same order of magnitude even after 100 h and 23 cycles. The increase in resistance with every cycle is also observed when thin films deposited onto bulk substrates are thermally cycled, although in

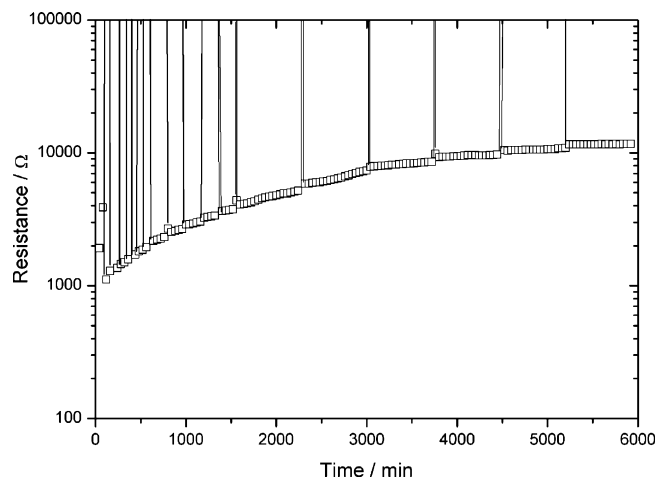


Fig. 7. Electrical resistance of thin films at 620  $^{\circ}\text{C}$  as a function of annealing time and cycling (vertical bars indicate rapid temperature cycles).

this case cycling is performed with only  $3\text{ }^{\circ}\text{C min}^{-1}$ . For these samples only a few thermal cycles have been done because each cycle takes 200 times longer compared to the micro-hotplate-based samples. Bending, mismatch in TEC and perhaps aging of the material become more important in thermal cycling than in long-term tests at constant temperature, thus degradation is faster during cycling. The unique ability of micro-hotplates to perform these fast temperature cycles creates the possibility to perform accelerated aging tests with placing heavy demands on the materials. This drastically speeds up degradation tests, which are otherwise very time consuming.

#### 4. Summary and conclusion

The feasibility to combine LSCF thin films, a typical SOFC cathode material, with micro-hotplates, a technology platform initially developed in the field of sensors, has been demonstrated in this work.

The micro-hotplates were able to withstand temperatures above  $800\text{ }^{\circ}\text{C}$ , which offers a secure margin to the target operating temperature of  $600\text{ }^{\circ}\text{C}$ .

The functionality of the LSCF thin film under these conditions was proven by obtaining the same electrical conductivity as for reference samples deposited onto bulk substrates. More rapid increase in the resistance of samples deposited onto micro-hotplates as a function of time was attributed to mismatch in TEC and bending of the micro-hotplate. Both might be diminished by using  $\text{Al}_2\text{O}_3$  instead of  $\text{SiN}$  as the membrane material, since  $\text{Al}_2\text{O}_3$  offers superior stiffness and a TEC closer to the values of LSCF and other fuel cell materials.

The integrated heater and the low heat capacity of the micro-hotplate allow fast heating rates up to  $10\text{ }^{\circ}\text{C s}^{-1}$  leading to short annealing times. After 5 min of annealing the film on the chip the microstructure did not change further even with longer annealing times. The conductivity data indicated that 30 min annealing on-chip leads to the same result as almost 4 h annealing on a bulk substrate, since the flexible membrane allows faster crystallization of the thin film.

When the integrated heater was used during film deposition, selective film growth in the heated areas only was obtained and thus no masking was required. However, flooding of the membrane from the surrounding spray solution outside the heated area has to be avoided.

In conclusion, the micro-hotplate is a suitable platform for micro-SOFC. Deposition of an electrolyte and anode as well as holes in the membrane for gas access would be the next steps to integrate a whole micro-SOFC on a micro-hotplate.

#### Acknowledgements

Financial support from the European network of excellence GOSPEL “General Olfaction and Sensing Projects on a Euro-

pean Level” under contract number IST-507610 and from Swiss Bundesamt für Energie under the project ONEBAT—Start and Kommission für Technik und Innovation ONEBAT Discovery Project are gratefully acknowledged. We would like to thank the IMT-Comlab technical staffs for their help in the processing of the devices.

#### References

- [1] D. Briand, A. Krauss, B. van der Schoot, U. Weimar, N. Barsan, W. Gopel, N.F. de Rooij, *Sens. Actuators B* 68 (2000) 223–233.
- [2] D. Barretino, M. Graf, W.H. Song, K.U. Kirstein, A. Hierlemann, H. Baltes, *IEEE J. Solid-State Circuit* 39 (2004) 1202–1207.
- [3] M. Heule, L.J. Gauckler, *Sens. Actuators B* 93 (2003) 100–106.
- [4] I. Simon, N. Barsan, M. Bauer, U. Weimar, *Sens. Actuators B* 73 (2001) 1–26.
- [5] D. Briand, S. Heimgartner, M.A. Grettillat, B. van der Schoot, N.F. de Rooij, *J. Micromech. Microeng.* 12 (2002) 971–978.
- [6] R.M. Tiggelaar, J.W. Berenschot, J.H. de Boer, R.G.P. Sanders, J.G.E. Gardeners, R.E. Oosterbroek, A. van den Berg, M.C. Elwenspoek, *Lab Chip* 5 (2005) 326–336.
- [7] W. Konz, J. Hildenbrand, M. Bauersfeld, S. Hartwig, A. Lambrecht, V. Lehmann, J. Wöllenstein, in: C. Cane, J.-C. Chiao, F.V. Verdu (Eds.), *Proceedings of Smart Sensors, Actuators, and MEMS II*, Sevilla, Spain, 2005, pp. 540–548.
- [8] C.H. Chen, H.J.M. Bouwmeester, H. Kruidhof, J.E. ten Elshof, A.J. Burggraaf, *J. Mater. Chem.* 6 (1996) 815–819.
- [9] P. Bohac, L.J. Gauckler, *Solid State Ionics* 119 (1999) 317–321.
- [10] I. Taniguchi, R.C. van Landschoot, J. Schoonman, *Solid State Ionics* 156 (2003) 1–13.
- [11] A. Bieberle-Hütter, D. Beckel, U.P. Muecke, J.L.M. Rupp, A. Infortuna, L.J. Gauckler, *Mstnews* 04/05 (2005) 12–15.
- [12] D. Beckel, A. Dubach, A.R. Studart, L.J. Gauckler, *J. Electroceram.* 16 (2006) 221–228.
- [13] D. Perednis, L.J. Gauckler, *J. Electroceram.* 14 (2005) 103–111.
- [14] MicroChem, 2006, [http://www.microchem.com/products/pdf/lor\\_data\\_sheet.pdf](http://www.microchem.com/products/pdf/lor_data_sheet.pdf).
- [15] L. Thiery, D. Briand, A. Odaymat, N.F. De Rooij, *Proceedings of International Workshops on Thermal Investigations of ICs and Systems*, Thermic, Sophia Antipolis, France, 2004, pp. 23–28.
- [16] D. Beckel, D. Briand, A.R. Studart, N.F. De Rooij, L.J. Gauckler, *Adv. Mater.* 18 (2006) 3105–3108.
- [17] U.P. Muecke, G.L. Messing, L.J. Gauckler, *Thin Solid Films*, submitted for publication.
- [18] J.F. Shackelford, W. Alexander, *CRC Materials Science and Engineering Handbook*, third ed., CRC Press, Boca Raton, 2001, p. 790.
- [19] D. Schneider, M.D. Tucker, *Thin Solid Films Papers presented at the 23rd International Conference on Metallurgical Coatings and Thin Films*, vols. 290–291, 1996, pp. 305–311.
- [20] D. Briand, F. Beaudoin, J. Courbat, N.F. De Rooij, R. Desplats, P. Perdu, *Microelectron. Reliab.* 45 (2005) 1786–1789.
- [21] J.L.M. Rupp, A. Infortuna, L.J. Gauckler, *Acta Mater.* 54 (2006) 1721–1730.
- [22] L.-W. Tai, M.M. Nasrallah, H.U. Anderson, D.M. Sparlin, S.R. Sehlin, *Solid State Ionics* 76 (1995) 273–283.
- [23] M.J. Madou, *Fundamentals of Microfabrication, The Science of Miniaturization*, second ed., CRC Press, Boca Raton, 2002, p. 300.
- [24] B.C.H. Steele, *Solid State Ionics* 75 (1995) 157–165.
- [25] J.F. Shackelford, W. Alexander, *CRC Materials Science and Engineering Handbook*, third ed., CRC Press, Boca Raton, 2001, p. 643.